First-principles calculations of gap bowing in $In_xGa_{1-x}N$ and $In_xAl_{1-x}N$ alloys: Relation to structural and thermodynamic properties

M. Ferhat[1,2] and F. Bechstedt[1]
[1]*Institut für Festkörpertheorie und Theoretische Optik, Friedrich-Schiller-Universität, 07743 Jena, Germany*
[2]*Département de Physique, Université des Sciences et de la Technologie d' Oran, Oran, Algeria*
(Received 28 September 2001; published 1 February 2002)

First-principles pseudopotential plane-wave calculations are used to investigate the electronic, structural, and thermodynamic properties of cubic nitride alloys $In_xGa_{1-x}N$ and $In_xAl_{1-x}N$. The alloys are described within a cluster-expansion method considering configurations in large 64-atom supercells. We find a strong composition-dependent gap bowing for both InGaN and InAlN alloys. The strongest contribution to the gap bowing is due to a structural effect, i.e., the composition-induced disorder in the bond lengths. Charge transfer is found to be important only for InAlN alloys. A small deviation from Vegard's law is found for the lattice parameter variation in InGaN and InAlN alloys. The calculated first- and second-nearest-neighbor distances in $In_xGa_{1-x}N$ alloys are in good agreement with the experimental data. The investigation of the thermodynamic stability of InGaN and InAlN alloys shows a significant tendency for spinodal decomposition.

DOI: 10.1103/PhysRevB.65.075213 PACS number(s): 61.66.Dk, 71.22.+i, 64.75.+g, 71.20.Nr

I. INTRODUCTION

Nitrogen-based III-V semiconductor compounds and alloys have attracted considerable interest in the last few years due to their applications in optoelectronics devices, for high-density optical data storage, and for high-power conversion. These devices can operate over a wide temperature range and remain unaffected by irradiation. An interesting feature of the device applications is generally the use of ternary $In_xGa_{1-x}N$ and $In_xAl_{1-x}N$ alloys.[1]

Extensive experimental and theoretical studies have addressed optical properties relevant to such technological applications. Unfortunately, however, there is still considerable disagreement about such fundamental parameters as the bowing of the fundamental energy gap. It is not clear how the band gap varies as a function of the alloy composition. Early optical studies of InGaN alloys suggested a small energy-gap bowing parameter.[2–4] Recent studies found a strong gap bowing in the range of 2–5 eV.[5–14] For InAlN, the scatter between different measurements of the band gap is significant. A large gap bowing was recently observed by Yamaguchi *et al.*,[15] a similarly strong bowing was found by Peng *et al.*,[16] and other workers measured a smaller bowing parameter.[17,18]

Partially these variations may be related to the absence of samples of high quality due to the fluctuations in the local indium molar fraction, the possible spinodal decomposition, and strain effects. The measured values of the band-gap bowing also depend on the technique of measurement of the band gap. Photoluminescence (PL) and absorption techniques give different values of the band gap of the ternary III-nitride alloys. A physical understanding of the mechanisms influencing the gap bowing is still missing.

In order to clarify the contradictory results we perform electronic-structure calculations based on first principles. The first goal of this paper is to understand the behavior of the gap bowing and to determine how it changes in a wide range of In molar fractions. In addition to the consideration of the electronic structure, we also address the more fundamental issue of atomic structure and phase stability of cubic InGaN and InAlN alloys and discuss their relationships to the bowing behavior.

The paper is organized as follows. In Sec. II we briefly explain the theoretical background of the electronic-structure calculations. Sec. III deals with results and their discussion. The paper is concluded in Sec. IV.

II. METHOD OF CALCULATION

The band-structure and total-energy calculations are performed using the first-principles density-functional theory (DFT) in the local-density approximation (LDA).[19] We use a plane-wave expansion of the eigenfunctions and non-norm-conserving *ab initio* Vanderbilt pseudopotentials implemented in the Vienna *ab initio* simulation package (VASP).[20] The Ga $3d$ and In $4d$ electrons are treated as valence electrons. Atomic relaxation is fully included for all alloy configurations studied.

A large 64-atom supercell representation is used in order to model the $In_xGa_{1-x}N$ and $In_xAl_{1-x}N$ alloys. More specifically, for the 64-atom $In_nX_{32-n}N_{32}$ supercells (X = Al or Ga), which correspond to $2\times2\times2$ conventional cubic cells, a zinc-blende lattice is assumed. For a given number $n = 0, \ldots, 32$ of In atoms, there are at least $\binom{32}{n}$ different atomic configurations that would have to be optimized structurally. This is impossible. Therefore, for a given number n of In atoms we usually study five different configurations in which the In atoms are not really randomly distributed. To guarantee the random character, we choose a more appropriate physical strategy. We begin with a maximum In-N clustered configuration; then we sequentially move the In atoms out of the cluster, to finally generate a minimum In-N clustered alloy (i.e., a maximum X-N clustered alloy).

For instance, in the $n=4$ case with 8 In and 24 X = Ga,Al atoms, the first configuration corresponds to two adjoining

8-atom cubes of InN. The average In-In distance represents a minimum. Then, we distribute the In atoms step by step over the other 8-atom cubes. In the fifth configuration each 8-atom cube contains one of the In atoms. Their distances are as far distant as possible. The band gap of the corresponding ordered alloy varies between the configurations. In the case of $In_8Al_{24}N_{32}$ the variation amounts to about 0.5 eV between the maximum and minimum clustered configurations. However, together with the probability of the occurrence of such a cluster configuration for a given average composition x the configurational average over all 37 $In_nX_{32-n}N_{32}$ cluster configurations under consideration gives a reasonable average fundamental gap of a random alloy $In_xX_{1-x}N$.

For each configuration j and each atomic number n, the fundamental physical properties (total energy, band gap, bond lengths, etc.) P_{nj} are determined. The configurationally averaged quantity $P(x)$ is computed using the Conolly-Williams approach,[21]

$$P(x)=\sum W_{nj}(x)P_{nj}. \tag{1}$$

The composition-dependent weights $W_{nj}(x)$ are determined for an ideal solid solution. They fulfill the constraints of normalization and definition of the average composition x, at least for the In molar fractions $x=0.25$, 0.5, and 0.75. Therefore, instead of calculating the quantities for the entire composition region we only use the $In_{8m}X_{8(4-m)}N_{32}$ clusters $(m=0,1,2,3,4)$. In the discussion the results are compared with those obtained for 8-atom clusters, in order to check the quality of the cluster-expansion method.[22]

III. RESULTS AND DISCUSSION

A. Electronic properties

Figures 1 and 2, respectively, show the calculated band-gap bowing coefficient for random InGaN and InAlN alloys, together with values of other theoretical work.[23–30] The calculations are based on the DFT-LDA, which should be a reasonable approximation[31] for the bowing in contrast to the gap itself. The aspect of spinodal decomposition into two random alloys within the miscibility gap is not taken into consideration. The calculated band-gap bowing parameter exhibits a strong composition dependence. This is different from conventional III-V alloys which show a weakly (<1 eV) composition-dependent bowing parameter. The calculated fundamental gap bowing for InGaN alloys ranges from 1.61 eV ($x=0.25$) to 1.26 eV ($x=0.75$), whereas for InAlN alloys it ranges from 4.67 eV ($x=0.25$) to 2.20 eV ($x=0.75$). Our results agree with the recent calculations of van Schilfgaarde *et al.*,[27] but small discrepancies with other calculations are obvious. The calculated bowing parameters, except of those of Bellaiche *et al.*[28] and Lambrecht,[25] are relatively small in comparison with measured values. Interesting is the comparison with similar cluster calculations,[29] which however are restricted to 8-atom supercells. The small supercells do not allow the local formation of small InN or XN ($X=$Ga or Al) clusters which may give rise to a substantial change in the gap value for a given In molar fraction with the consequences for the bowing parameter shown in Fig. 1.

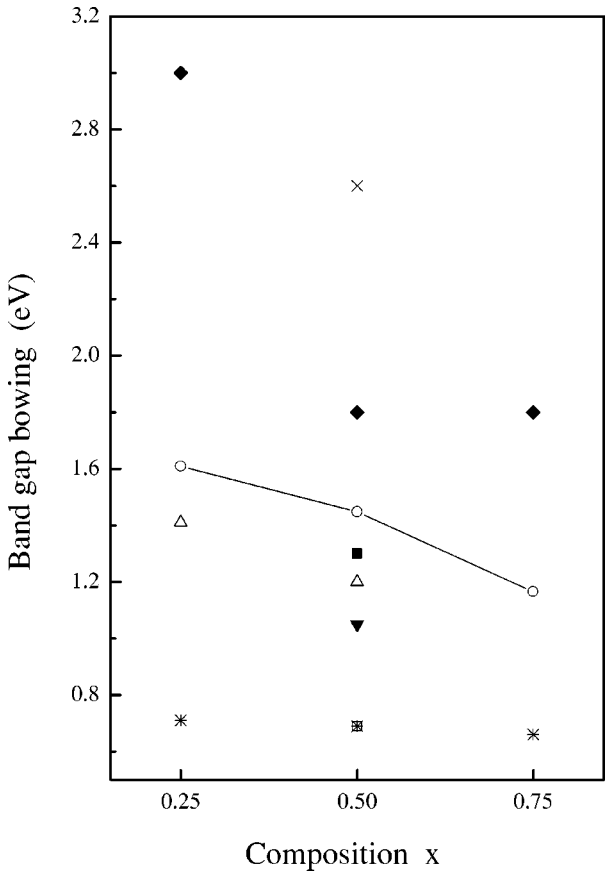

FIG. 1. Composition dependence of the calculated band gap bowing (open circles) for InGaN alloys, compared to other theoretical values. Reference 28: solid diamonds. Reference 30: open triangles. Reference 29: star. Reference 25: cross. Reference 27: solid square. Reference 26: open squares. Reference 23: solid triangles.

The extraction of the gap bowing parameter of InGaN and InAlN from the various optical measurements requires knowledge of the band gaps of the binary compounds GaN, AlN, and InN. While the band gap of GaN and AlN is well known today, the band structure of InN is rather uncertain, because of sample-quality problems. Usually a value of about 1.9 eV (Ref. 32) is considered as the fundamental gap. However, recent studies suggest a smaller gap. O'Donnell[33] measured peak positions in the photoluminescence spectrum at about 1.7 eV for $In_xGa_{1-x}N$ alloys with an In concentration of only $x=0.4$ far away from $x=1$. Similar results were found by Yamaguchi *et al.*,[15] who measured the peak position of the PL at about 1.66 eV for $In_xAl_{1-x}N$ alloys for $x=0.6$. Optical absorption and photoluminescence measurements of high-quality samples, as well as quasiparticle calculations beyond DFT-LDA, seem to tend to InN energy gaps close to 1 eV.[34] More reliable experimental studies are highly desirable, since a lower value of the band gap of InN will dramatically reduce the difference between bowing parameters determined experimentally or theoretically.

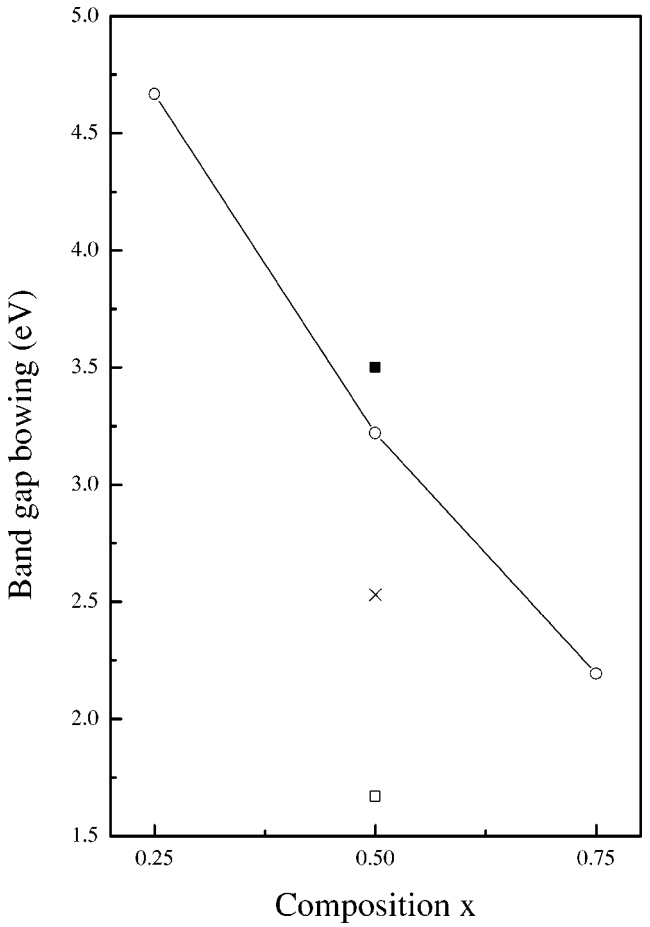

FIG. 2. Composition dependence of the calculated band gap bowing (open circles) for InAlN alloys, compared to other theoretical values. Reference 27: solid square. Reference 24: cross. Reference 26: open squares.

In order to better understand the physical origins of the large and composition-dependent bowing in $In_xGa_{1-x}N$ and $In_xAl_{1-x}N$ alloys, we follow the procedure of Bernard and Zunger[35] and decompose the total bowing parameter b into physically distinct contributions. The overall bowing coefficient at a given average composition x measures the change in band gap according to the formal reaction

$$x\mathrm{InN}(a_{\mathrm{InN}})+(1-x)X\mathrm{N}(a_{X\mathrm{N}})\rightarrow \mathrm{In}_xX_{1-x}\mathrm{N}(a_{\mathrm{eq}}), \quad (2)$$

where a_{InN} and $a_{X\mathrm{N}}$ are the equilibrium lattice constants of the binary compound InN and XN, respectively. a_{eq} is the equilibrium lattice constant of the alloy with the average composition x.

We decompose reaction (2) into three steps:

$$\mathrm{InN}(a_{\mathrm{InN}})+X\mathrm{N}(a_{X\mathrm{N}})\rightarrow \mathrm{InN}(a)+X\mathrm{N}(a), \quad (3)$$

$$x\mathrm{InN}(a)+(1-x)X\mathrm{N}(a)\rightarrow \mathrm{In}_xX_{1-x}\mathrm{N}(a), \quad (4)$$

$$\mathrm{In}_xX_{1-x}\mathrm{N}(a)\rightarrow \mathrm{In}_xX_{1-x}\mathrm{N}(a_{\mathrm{eq}}). \quad (5)$$

The first step measures the volume deformation (VD) effect on the bowing. The corresponding contribution b_{VD} to the total bowing parameter represents the relative response of the band structure of the binary compounds InN and XN to hydrostatic pressure, which here arises from the change of their individual equilibrium lattice constants to the alloy value $a=a(x)$. The second contribution, the charge exchange (CE) contribution b_{CE}, reflects a charge transfer effect which is due to the different (averaged) bonding behavior at the lattice constant a. The final step, the ''structural relaxation'' (SR), measures changes in passing from the unrelaxed to the relaxed alloy by b_{SR}. Consequently, the total bowing parameter is defined as

$$b=b_{\mathrm{VD}}+b_{\mathrm{CE}}+b_{\mathrm{SR}}. \quad (6)$$

TABLE I. Calculated bowing parameters b for InGaN (InAlN) alloys. The contributions due to volume deformation (b_{VD}), electronegativities (b_{CE}), and structural relaxations (b_{SR}) are also listed. All values are in eV.

Composition x	0.25	0.50	0.75
b_{VD}	1.41 (2.68)	1.32 (2.45)	1.29 (2.25)
b_{CE}	0.11 (1.88)	−0.02 (0.69)	−0.29 (−0.41)
b_{SR}	0.09 (0.11)	0.12 (0.09)	0.26 (0.36)
b	1.61 (4.67)	1.42 (3.23)	1.26 (2.20)

The general representation of the composition-dependent band gap of the alloys in terms of the gaps of the binary compounds, $E_{\mathrm{InN}}(a_{\mathrm{InN}})$ and $E_{X\mathrm{N}}(a_{X\mathrm{N}})$, and the total bowing parameter b is

$$E_g(x)=xE_{\mathrm{InN}}(a_{\mathrm{InN}})+(1-x)E_{X\mathrm{N}}(a_{X\mathrm{N}})-bx(1-x). \quad (7)$$

This allows a division of the total bowing b into three contributions according to

$$b_{\mathrm{VD}}=\frac{E_{\mathrm{InN}}(a_{\mathrm{InN}})-E_{\mathrm{InN}}(a)}{1-x}+\frac{E_{X\mathrm{N}}(a_{X\mathrm{N}})-E_{X\mathrm{N}}(a)}{x}, \quad (8)$$

$$b_{\mathrm{CE}}=\frac{E_{\mathrm{InN}}(a)}{1-x}+\frac{E_{X\mathrm{N}}(a)}{x}-\frac{E_{\mathrm{In}X\mathrm{N}}(a)}{x(1-x)}, \quad (9)$$

$$b_{\mathrm{SR}}=\frac{E_{\mathrm{In}X\mathrm{N}}(a)-E_{\mathrm{In}X\mathrm{N}}(a_{\mathrm{eq}})}{x(1-x)}. \quad (10)$$

All these energy gaps occurring in expressions (8)–(10) have been calculated for the indicated atomic structures and lattice constants. The bowing coefficients b calculated at In molar fractions $x=0.25$, 0.50, and 0.75 are listed in Table I for InGaN and InAlN alloys, together with three contributions b_{VD} [Eq. (8)], b_{CE} [Eq. (9)], and b_{SR} [Eq. (10)] due to volume deformation, different atomic electronegativities, and structural relaxation. We observe the following facts.

(i) The volume-deformation term b_{VD} of InGaN and InAlN alloys is large, particularly for InAlN. The importance of b_{VD} can be correlated to the large mismatch of the lattice constants of the corresponding binary compounds ($\approx 10\%$ between GaN and InN and $\approx 14\%$ between AlN and InN). Thus, the b_{VD} term, i.e., the composition-induced disorder in the bond lengths, appears to control the large gap bowing in InGaN and InAlN alloys.

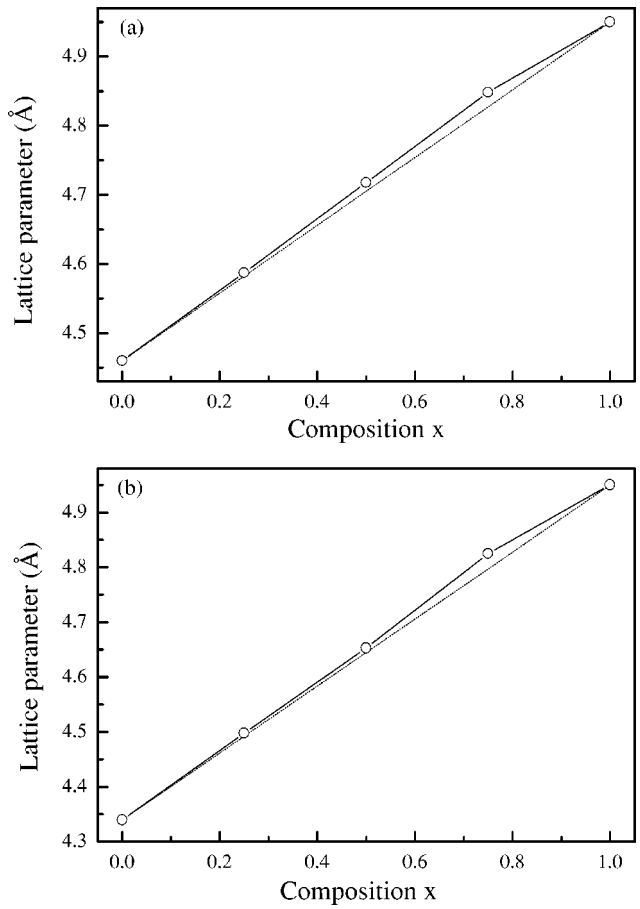

FIG. 3. Lattice constants of InGaN (a) and InAlN (b) vs composition (open circles) compared to the virtual crystal approximation (VCA) (dashed line).

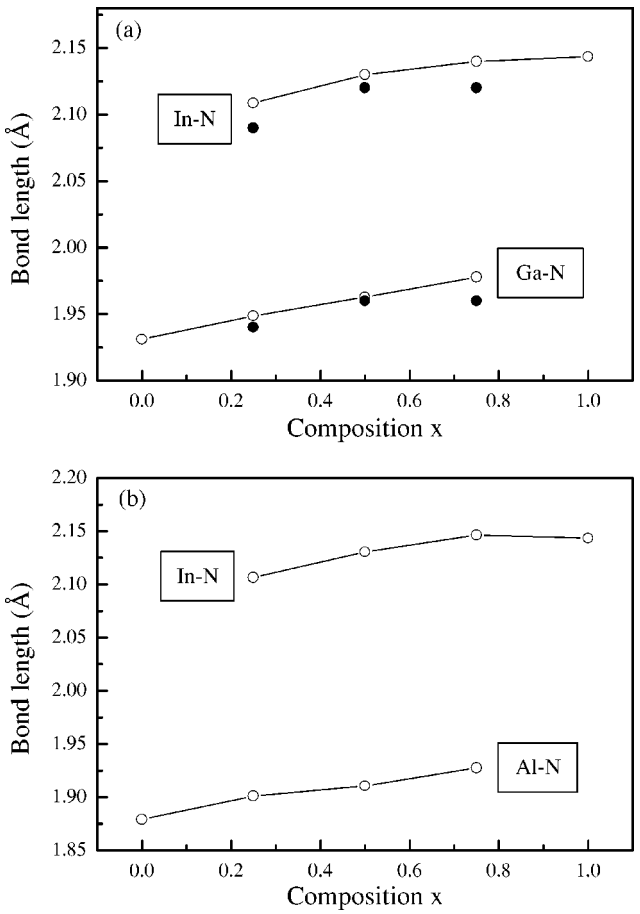

FIG. 4. Averaged bond lengths in InGaN (a) and InAlN (b) alloys vs composition (open circles) compared to the experimental data (solid cirles, Ref. 38).

(ii) The charge-transfer contribution b_{CE} due to the different electronegativities of the In and X (X=Al or Ga) atoms is considerable for InAlN alloys but small for InGaN alloys. Indeed, b_{CE} scales with the electronegativity mismatch [$\approx$2% ($\approx$13%), between In and Ga (In and Al) using Pauling's scale[36]]. This term governs the composition dependence of the bowing in the case of InAlN.

(iii) The contribution of the structural relaxation b_{SR} is small for both alloys under consideration. Such a weak effect has also been found by Wei and Zunger,[37] studying mixed-anion alloys (e.g., GaAsN). They also show a stronger structural effect on the gap bowing than mixed-cation alloys (e.g., GaInAs). The principal static atomic displacement in mixed-cation alloys with respect to the ideal zinc-blende position is due to anion displacement, while in mixed-anion alloys the principal displacement is due to the cation. The cation displacements lead to strong intraband coupling within the conduction band and separately within the valence band; consequently the cation displacements lower the band gap considerably more than anion displacements.

B. Structural properties

The three different contributions due to the gap bowing are related to the atomic structure, in particular, to the bond lengths and second-nearest-neighbor (2NN) distances. The corresponding information is given in Figs. 3–5. Figures 3(a) and 3(b) show the variation of the calculated equilibrium lattice constant versus In concentration for InGaN and InAlN alloys, respectively. A small deviation from Vegard's law is clearly visible, in particular for large In molar fractions $x \approx 0.8$. This is slightly in contrast to calculations using 8-atom clusters.[22] The reason is that within large supercells the local InN regions tend to have large lattice constants. We are not aware of any experimental data indicating how closely the lattice constant follows Vegard's law in InGaN and InAlN alloys. However, similar theoretical results for InGaN alloys were recently published by Lambrecht.[25] The physical origin of this small deviation should be mainly due to the large mismatch of the lattice constants of InN and XN compounds. Figures 4(a) and 4(b) show the calculated bond lengths of $R_{\text{In-N}}, R_{\text{Ga-N}}$ and $R_{\text{In-N}}, R_{\text{Al-N}}$ in InGaN and InAlN, respectively, as a function of the In molar fraction together with the recent results obtained by means of an x-ray absorption fine structure (EXAFS) technique.[38] We find good agreement between the calculated and experimental values for InGaN alloys. The quality of agreement is not much better as in the case of 8-atom cells, indicating that structural properties can be reasonably described within the smaller cells. The predicted bond lengths reveal a weak almost linear dependence

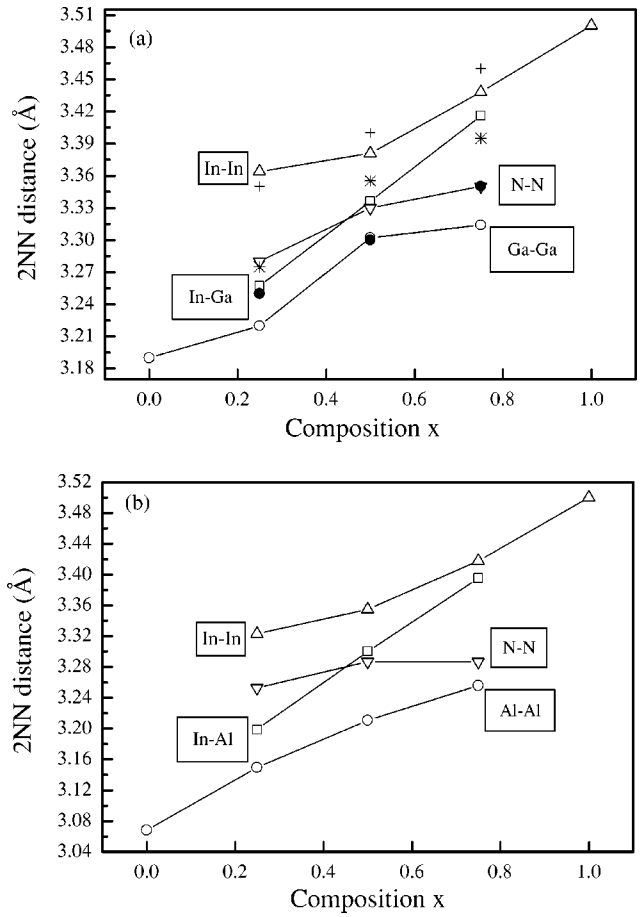

FIG. 5. Averaged second-nearest-neighbor distances in InGaN (a) and InAlN (b) alloys vs composition compared to the experimental data. Reference 38: In-In (cross), In-Ga (star), Ga-Ga (solid circles).

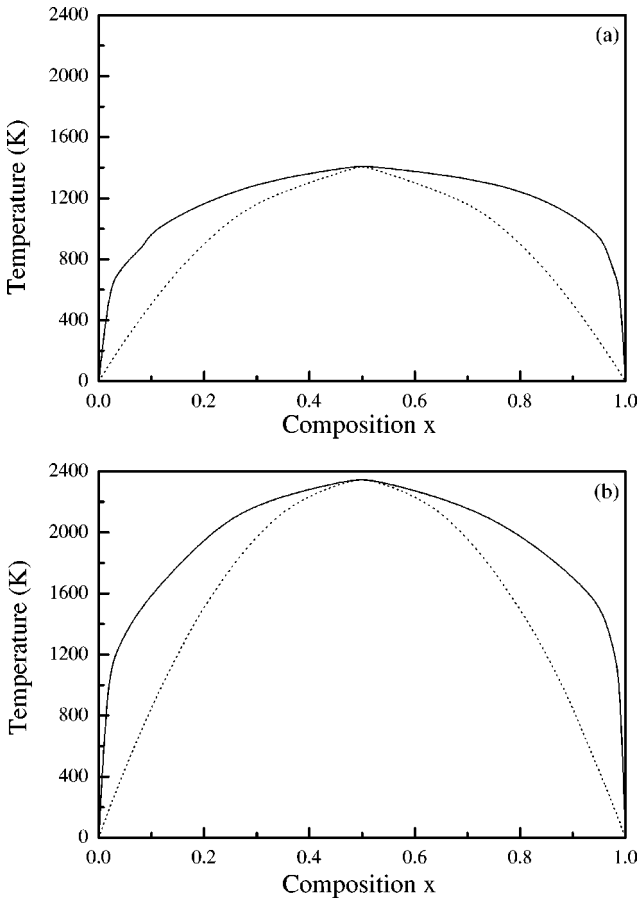

FIG. 6. *T*-*x* phase diagram of InGaN (a) and InAlN (b) alloys. Solid line: binodal curve. Dashed line: spinodal curve.

on the alloy composition. $R_{\text{In-N}}, R_{\text{Ga-N}}$ and $R_{\text{In-N}}, R_{\text{Al-N}}$ do not deviate substantially from their natural values in the corresponding binary compounds; the distribution is bimodal. The individual identities of In-N and *X*-N bonds are preserved in the alloys; the accommodations of their natural differences occur elsewhere. The cation-cation-related splitting (In-N vs *X*-N) is much larger for bonds in InAlN than those in InGaN alloys (0.22 Å vs 0.16 Å) due to the large size mismatch between the binary constituents AlN vs InN than compared with GaN vs InN. These results make obvious that, in contrast to the lattice constants, Vegard's law fails for bond lengths of both InGaN and InAlN as in other III-V alloys. The second-nearest-neighbor distances are plotted in Fig. 5 for InGaN and InAlN. Again good agreement with experimental data can be stated for InGaN alloys, in particular taking into account the uncertainties due to length fluctuations. The In-In, N-N, In-*X*, and *X*-*X* distances shown in Fig. 5 exhibit four distinct values: the smallest distance is found for the *X*-*X* value (Ga-Ga and Al-Al), while the In-In distance is the largest, and the N-N and In-*X* lengths are between the two extremes. We also note that the dependence on composition for the cation-cation 2NN distances is significantly larger than for the nearest-neighbor bonds. The hetero second-nearest-neighbor distances $R_{\text{In-Ga}}$ and $R_{\text{In-Al}}$ exhibit a stronger composition dependence than the second-nearest-neighbor distances $R_{\text{Ga-Ga}}$, $R_{\text{In-In}}$, and $R_{\text{Al-Al}}$ of equal cations. This feature differs from those observed in other III-V alloy systems, where all the second NN cation-cation distances almost follow the same composition dependence.[39]

C. Thermodynamic properties

The properties of the mixed crystals InGaN and InAlN studied experimentally are not only influenced by composition fluctuations on an atomic length scale but also by decomposition into different random alloys for not too small and not too large In molar fractions. Information about such a miscibility gap follows from the free energy of the mixed ternary system. An important contribution arises from the mixing enthalpy. The mixing enthalpy of $\text{In}_x X_{1-x}\text{N}$ alloys can be obtained from the calculated total energies as

$$\Delta H = E_{\text{In}X\text{N}} - xE_{\text{InN}} - (1-x)E_{X\text{N}}, \tag{11}$$

where $E_{\text{In}X\text{N}}$, E_{InN}, and $E_{X\text{N}}$ are the respective total energies for In*X*N alloys, InN, and *X*N. For $x = 0.5$ we find 34 meV/atom for the InGaN alloy and 53 meV/atom for the InAlN alloy. The large values of ΔH for InGaN and InAlN alloys suggest large critical temperatures. Consequently, there will be a tendency for immiscibility in a wide composition range at temperatures *T* of epitaxial growth. The larger mixing

enthalpy for InAlN alloys suggests a higher critical temperature and, hence, that the immiscibility tendency is more prounouced.

From the resulting free energy of mixing, $\Delta F = \Delta H - RT[x \ln x + (1-x)\ln(1-x)]$, where R is the gas constant, we calculate the temperature-composition phase diagrams which show the stable, metastable, and unstable composition regions of a mixed crystal for a given growth temperature. Figure 6 depicts the calculated phase diagrams for InGaN and InAlN alloys. We observe a critical temperature of 1400 K for InGaN alloys and 2350 K for InAlN alloys. The use of smaller 8-atom supercells gives rise to slightly smaller critical temperatures, in particular in the InAlN case.[40] The higher critical temperature of InAlN compared to InGaN can be understood in the light of the larger lattice mismatch of the binary compounds AlN and InN. The mismatch in the lattice parameters of the binary InN and XN leads to the existence of an extended miscibility gap accompanied by spinodal decomposition. Our results for InGaN widely agree with the calculation of Saito and Arakawa,[41] who used the valence-force-field method and found a critical temperature of about 1417 K. Our results indicate that for intermediate compositions InGaN and InAlN alloys are unstable at the temperatures commonly used in epitaxial growth. This is in agreement with the fact that recent experimental work[42,43] reported strong evidence of phase separation for InGaN alloys. In the case of spinodal decomposition the band gap and its bowing behavior has to be discussed carefully in the dependence on the measurement method used.

IV. CONCLUSIONS

In summary, we have studied the electronic, structural, and thermodynamic properties of $In_xGa_{1-x}N$ and $In_xAl_{1-x}N$ alloys by performing first-principles pseudopotential plane-wave calculations. We found a strong composition dependence of the gap bowing of InGaN and InAlN alloys. Our results suggest that the bowing of InAlN alloys have a remarkable contribution from the structural (volume deformation) effect and it is also characterized by an important charge-transfer effect. On the other hand, the gap bowing of InGaN alloys is dominated by the structural effect. The lattice constants of InGaN and InAlN follow Vegard's law, but small deviations occur for large In molar fractions around $x = 0.8$. The bond lengths and the second-nearest-neighbor distances calculated for InGaN alloys are in good agreement with data obtained from recent x-ray absorption fine structure measurements. The hetero second-nearest-neighbor distances in InGaN and InAlN alloys show stronger composition dependences than the second-nearest-neighbor distances between like atoms. The calculated phase diagrams indicate a significant phase miscibility gap. The calculated critical temperatures are 1400 K and 2350 K, respectively, for InGaN and InAlN alloys. These results indicate that InGaN and InAlN alloys are unstable over a wide range of intermediate compositions at normal growth temperatures. This effect has also to be taken into account in the discussion of the gap bowing.

ACKNOWLEDGMENTS

We are grateful to J.-M. Wagner for a careful reading of the manuscript and valuable discussions. We thank J. Furthmüller for the assistance with the computer code VASP. This work is supported by the Deutsche Forschungsgemeinschaft (Schwerpunktprogramm ''Gruppe III-Nitride,'' Project No. Be1346/8-5) and the Islamic Development Bank (Jeddah, Kingdom of Saudi Arabia).

[1] S. Nakamura and G. Fasol, *The Blue Laser Diode* (Springer, Berlin, 1997).
[2] K. Osamura, S. Naka, and Y. Marukami, J. Appl. Phys. **46**, 3432 (1975).
[3] T. Nagatomo, T. Kuboyama, H. Minamino, and O. Omoto, Jpn. J. Appl. Phys., Part 2 **28**, L1334 (1989).
[4] N. Yoshimoto, T. Matsuoka, and A. Katsui, Appl. Phys. Lett. **59**, 2251 (1991).
[5] M.D. McCluskey, C.G. Van de Walle, C.P. Master, L.T. Romano, and N.M. Johnson, Appl. Phys. Lett. **72**, 2725 (1998).
[6] C.A. Parker, J.C. Roberts, S.M. Bedair, M.J. Reed, S.X. Liu, N.A. El-Masry, and L.H. Robins, Appl. Phys. Lett. **75**, 2566 (1999).
[7] C. Wetzel, T. Takeuchi, S. Yamaguchi, H. Katch, H. Amano, and I. Akasaki, Appl. Phys. Lett. **73**, 1994 (1998).
[8] W. Shan, B.D. Little, J.J. Song, Z.C. Feng, M. Schurman, and R.A. Stall, Appl. Phys. Lett. **69**, 3315 (1996).
[9] T. Takeuchi, H. Takeuchi, S. Sota, H. Sakai, H. Amano, and I. Akasaki, Jpn. J. Appl. Phys., Part 2 **36**, L177 (1997).
[10] W. Shan, W. Walukiewizc, E.E. Haller, B.D. Little, J.J. Song, M.D. McCluskey, N.M. Johnson, Z.C. Feng, M. Schurman, and R.A. Stall, J. Appl. Phys. **84**, 4452 (1998).
[11] O. Brandt, J.R. Müllhäuser, B. Yang, H. Yang, and K.H. Ploog, Physice E (Amsterdam) **2**, 532 (1998).
[12] J. Wagner, A. Ramakrishnan, D. Behr, M. Maier, N. Herres, M. Kunzer, H. Obloh, and K.-H. Bachem, MRS Internet J. Nitride Semicond. Res. **4S1**, G2.8 (1999).
[13] H.P.D. Schenk, P. de Mierry, M. Laügt, F. Omnes, M. Lerous, B. Beaumont, and P. Gibart, Appl. Phys. Lett. **75**, 2587 (1999).
[14] R. Goldhahn, J. Scheiner, S. Shokhovets, T. Frey, U. Köhler, D.J. As, and K. Lischka, Appl. Phys. Lett. **76**, 291 (2000).
[15] S. Yamaguchi, M. Kariya, S. Nitta, T. Takeuchi, C. Wetzel, H. Amano, and I. Akasaki, Appl. Phys. Lett. **76**, 876 (2000).
[16] T. Peng, J. Piprek, G. Qui, J.O. Olowolafe, K.M. Unruh, C.P. Swann, and E.F. Schubert, Appl. Phys. Lett. **71**, 2439 (1997).
[17] M.J. Lukitsch, Y.V. Danylyuk, V.M. Naik, C. Huang, G.W. Auner, L. Rimai, and R. Naik, Appl. Phys. Lett. **79**, 632 (2001).
[18] K.S. Kim, A. Saxler, P. Kung, M. Razeghi, and K.Y. Lim, Appl. Phys. Lett. **71**, 800 (1997).
[19] P. Hohenberg and W. Kohn, Phys. Rev. **136**, 864 (1964).
[20] G. Kresse and J. Furthmüller, Comput. Mater. Sci. **6**, 15 (1996); Phys. Rev. B **54**, 11 169 (1996).
[21] J.W.D. Conolly and A.R. Williams, Phys. Rev. B **27**, 5169 (1983).

[22] L.K. Teles, J. Furthmüller, L.M.R. Scolfaro, J.R. Leite, and F. Bechstedt, Phys. Rev. B **62**, 2475 (2000).
[23] A.F. Wright and J.S. Nelson, Appl. Phys. Lett. **66**, 3465 (1995).
[24] A.F. Wright and J.S. Nelson, Appl. Phys. Lett. **66**, 3051 (1995).
[25] W.R.L. Lambrecht, Solid-State Electron. **41**, 195 (1997).
[26] K. Kim, S. Limpijumnong, W.R.L. Lambrecht, and B. Segall, in *III.-V Nitrides*, edited by F. A. Ponce, T. D. Moustakas, I. Akasaki, and B. A. Monemar, Mater. Res. Soc. Symp. Proc. No. 449, (Material, Research Society, Pittsburgh 1997), p. 926.
[27] M. van Schilfgaarde, A. Sher, and A.-B. Chen, J. Cryst. Growth **178**, 8 (1997).
[28] L. Bellaiche, T. Mattila, L.-W. Wang, S.-H. Wei, and A. Zunger, Appl. Phys. Lett. **74**, 1842 (1999).
[29] L.K. Teles, J. Furthmüller, L.M.R. Scolfaro, J.R. Leite, and F. Bechstedt, Phys. Rev. B **63**, 085204 (2001).
[30] A.F. Wright, K. Leung, and M. van Schilfgaarde, Appl. Phys. Lett. **78**, 189 (2001).
[31] S.-H. Wei, L.G. Ferreira, J.E. Bernard, and A. Zunger, Phys. Rev. B **42**, 9622 (1990).
[32] T.L. Tansley and C.P. Foley, J. Appl. Phys. **59**, 3241 (1986).
[33] K.P. O'Donnell, Phys. Status Solidi A **183**, 117 (2001).
[34] V. Yu. Davydov, A. A. Klochikhin, R. P. Seisyan, V. V. Emtsev, S. V. Ivanov, F. Bechstedt, J. Furthmüller, H. Harima, and A. V. Mudriy, Phys. Status Solidi B **229,** R1 (2002).
[35] J.E. Bernard and A. Zunger, Phys. Rev. B **36**, 3199 (1987).
[36] W. Sargent, *Table of Periodic Properties of the Elements* (Sargent-Welch Scientific, Skokie, IL, 1980).
[37] S.-H. Wei and A. Zunger, Phys. Rev. Lett. **76**, 664 (1996).
[38] N.J. Jeffs, A.V. Blant, T.S. Cheng, C.T. Foxon, C. Bailey, P.G. Harrison, A.J. Dent, and J.F.W. Mosselmans, in *Wide-Bandgap Semiconductors for High Power, High Frequency and High Temperature*, edited by S. Den Baars, M. S. Shar, J. Palmour, and M. Spencer, Mater. Res. Soc. Symp. Proc. No. 512 (Material, Research Society, Pittsburgh, 1998), p. 519.
[39] J.C. Mikkelsen and J.B. Boyce, Phys. Rev. B **28**, 7130 (1983).
[40] L. K. Teles, J. Furthmüller, L. M. R. Scolfaro, J. R. Leite, F. Bechstedt, T. Frey, D. J. As, and K. Lischka, Physica E (to be published).
[41] T. Saito and Y. Arakawa, Phys. Rev. B **60**, 1701 (1999).
[42] E. Silveira, A. Tabata, J.R. Leite, R. Truti, V. Lemos, T. Frey, D.J. As, D. Schikora, and K. Lischka, Appl. Phys. Lett. **72**, 40 (1998).
[43] N.A. El-Masry, E.L. Piner, S.X. Liu, and S.M. Bedair, Appl. Phys. Lett. **72**, 40 (1998).